Altered phenotype in LMAN1-deficient mice with low levels of residual LMAN1 expression

Lesley A. Everett,[1] Rami N. Khoriaty,[2-5] Bin Zhang,[6] and David Ginsburg[1,2,7,8]

[1]Department of Human Genetics, University of Michigan Medical School, Ann Arbor, MI; [2]Department of Internal Medicine, [3]Department of Cell and Developmental Biology, and [4]Cellular and Molecular Biology Program, University of Michigan, Ann Arbor, MI; [5]University of Michigan Rogel Cancer Center, Ann Arbor, MI; [6]Genomic Medicine Institute, Lerner Research Institute, Cleveland Clinic, Cleveland, OH; [7]Department of Pediatrics and Communicable Diseases, University of Michigan, Ann Arbor, MI; and [8]Howard Hughes Medical Institute, Chevy Chase, MD

Key Points

- There is a dose–response relationship between *Lman1* expression level and secretion levels of LMAN1 cargoes in mice (FV, FVIII, and A1AT).

- Therapeutic targeting of LMAN1 to reduce FV and FVIII as an anticoagulant strategy may only require partial inhibition of LMAN1 function.

Combined deficiency of coagulation factors V and VIII (F5F8D) is an autosomal recessive bleeding disorder caused by loss-of-function mutations in either *LMAN1* or *MCFD2*. The latter genes encode 2 components of a mammalian cargo receptor that facilitates secretion of coagulation factor V (FV) and factor VIII (FVIII) from the endoplasmic reticulum (ER) to the Golgi via coat protein complex II vesicles. F5F8D patients exhibit FV and FVIII levels that are ~10% to 15% of normal. We report herein a comparative analysis for a series of murine *Lman1* alleles. Consistent with previous reports, mice completely deficient in LMAN1 (*Lman1*$^{-/-}$) exhibit ~50% FV and FVIII levels. In contrast, mice carrying a hypomorphic *Lman1* allele (*Lman1*$^{cgt/cgt}$) that expresses ~6% to 8% of wild-type *Lman1* mRNA levels exhibit intermediate plasma FV and FVIII reductions (~70% of wild-type levels). *Lman1*$^{-/-}$ mice exhibit ER accumulation of another LMAN1 cargo, alpha-1 antitrypsin (A1AT), with an intermediate level of A1AT ER retention observed in *Lman1*$^{cgt/cgt}$ mice. Finally, the previously reported strain-specific, partially penetrant, perinatal lethality of LMAN1-deficient mice (*Lman1*$^{gt1/gt1}$) was confirmed in *Lman1*$^{-/-}$ mice, although it was not observed in *Lman1*$^{cgt/cgt}$ mice. Taken together, these results show a dose-dependent effect of residual LMAN1 on the secretion of its cargo proteins. The results also suggest that human subjects with hypomorphic *LMAN1* mutations might present with mild bleeding phenotypes resulting from more modest reductions in FV and FVIII, which could be missed by routine clinical evaluation. Finally, these findings suggest that therapeutic targeting of LMAN1 to reduce FV and FVIII as an anticoagulant strategy may only require partial inhibition of LMAN1 function.

Introduction

The LMAN1/MCFD2 cargo receptor is required for efficient secretion of coagulation factors V (FV) and VIII (FVIII).[1] FV is synthesized in hepatocytes[2,3] (humans and mice) and megakaryocytes[4] (mice), whereas FVIII is synthesized exclusively by endothelial cells.[5,6] Human mutations in either *LMAN1* or *MCFD2* cause combined deficiency of coagulation FV and FVIII (F5F8D), an autosomal recessive bleeding disorder characterized by reduction of both FV and FVIII to ~10% to 15% of normal levels.[7,8]

LMAN1 is a type 1 transmembrane protein that cycles between the endoplasmic reticulum (ER) and the ER Golgi intermediate compartment (ERGIC) in the mammalian secretory pathway; it belongs to a family of homologous L-type mannose-binding lectins that function in the trafficking of *N*-linked glycoproteins.[9-11] LMAN1 contains an ER luminal carbohydrate recognition domain that binds

---

cargo proteins,[12,13] as well as a short cytosolic tail that interacts with the SEC24 component of the coat protein complex II vesicle coat (for anterograde transport to the ERGIC).[14,15] LMAN1 forms a 1:1 complex with MCFD2, and together these proteins function as a cargo receptor complex. Approximately 70% of human F5F8D patients exhibit mutations in *LMAN1*, with the remainder in *MCFD2*.[16] Nearly all reported human *LMAN1* mutations are null mutations predicted to result in complete absence of the LMAN1 protein, with 2 interesting exceptions that are missense mutations (W67S and C475R) resulting in disruption of protein oligomerization and protein structural integrity.[7,13,17-21] The marked preponderance of null *LMAN1* mutations in F5F8D patients suggests that even small residual levels of *LMAN1* expression may be sufficient to maintain physiological levels of FV and FVIII secretion.

LMAN1 and MCFD2 are ubiquitously expressed, and their orthologs are present in invertebrates (including Caenorhabditis *elegans*) before the appearance of FV and FVIII, suggesting a broader role for LMAN1 in protein secretion. Other potential LMAN1 secretory cargoes include alpha-1 antitrypsin (A1AT),[22] cathepsin C,[23] cathepsin Z,[24] Mac-2 binding protein,[25] matrix metalloproteinase-9,[26] and γ-aminobutyric acid type A receptors.[27] Among these potential cargo proteins, only A1AT has been confirmed in vivo (in the mouse),[28] although γ-aminobutyric acid type A receptors are decreased in LMAN1-deficient mouse brain.[27] In addition, LMAN1 has been implicated in the production of infectious particles from several highly pathogenic RNA virus families[29] and may also contribute to photoreceptor homeostasis.[30] Furthermore, mutations resulting in *LMAN1* inactivation have been identified at high frequencies in colorectal tumors with microsatellite instability.[31]

Mice homozygous for a gene trap insertion in *Lman1* intron 10 (*Lman1*[gt1/gt1]) exhibit FV and FVIII activity levels that are reduced to ~50% of wild-type littermate levels.[28] These mice also exhibit retention of A1AT in the hepatocyte ER, with normal steady-state plasma A1AT levels in female mice and only a slight reduction in plasma A1AT levels in male mice.[28,32] The less severe reductions of FV and FVIII in *Lman1*[gt1/gt1] mice relative to those of F5F8D humans could be explained by low levels of residual LMAN1 expression from the gene trap allele, or differences in FV and FVIII secretion between mice and humans. *Lman1*[gt1/gt1] mice also exhibit a partially penetrant, perinatal lethality that is restricted to certain genetic strain backgrounds.[28] In contrast, *Mcfd2*^{−/−} mice exhibit slightly lower FV and FVIII levels than *Lman1*[gt1/gt1] mice but no perinatal lethality.[32]

We report here an analysis of mice homozygous for a second, independent *Lman1* null allele with complete LMAN1 deficiency (*Lman1*^{−/−}), as well as hypomorphic LMAN1-deficient mice (*Lman1*[cgt/cgt]) that retain ~7% of normal *Lman1* expression. We describe a dose–response relationship between the level of *Lman1* gene expression and the secretion of LMAN1 cargoes, suggesting that LMAN1 may be a potential therapeutic target for anticoagulation. We also confirm a strain-specific, perinatal lethality in LMAN1-deficient mice, indicating that additional LMAN1-dependent secretory cargoes remain to be identified.

Methods

Lman1 and *Mcfd2* mutant mice

Lman1[gt1] mice carrying a gene trap insertion in *Lman1* intron 10 (Figure 1A) were described previously[28] and are maintained on

a C57BL/6J genetic background. Polymerase chain reaction (PCR) genotyping for the *Lman1*[gt1] allele was performed as previously described.

Lman1[cgt] (Figure 1B) and *Lman1*[fl] (Figure 1C) mice were previously described[5] and are maintained on a C57BL/6J genetic background. The *Lman1*[fl] allele was converted to the null *Lman1*^{−} allele [*Lman1*[tm1d(KOMP)Wtsi]] (Figure 1D) by *Cre*-mediated excision of exons 2 and 3. Transgenic C57BL/6J mice carrying *Cre* recombinase driven by a ubiquitous *EIIA* promoter [B6.FVB-Tg(EIIa-cre)C5379Lmgd/J; stock no. 003724] were obtained from The Jackson Laboratory, as were 129S1/SvlmJ mice (stock no. 002448). Primer trio A/B/C was used to distinguish between the *Lman1*^{+}, *Lman1*[cgt], and *Lman1*^{−} alleles (Figure 1E) as previously described[5] with the primers listed in Table 1. *Mcfd2*^{−} mice were previously generated by deleting exons 2 and 3 of the *Mcfd2* gene,[32] with genotyping performed as previously described. The *Mcfd2*^{−} allele was maintained on a C57BL/6J genetic background. To assess *Lman1*^{−/−} lethality on a mixed genetic background, *Lman1*^{+/−} F1 mice were generated [by crossing an *Lman1*^{+/−} mouse on C57BL/6J strain to a wild-type (*Lman1*^{+/+})129S1/SvlmJ mouse] and subsequently intercrossed to produce F2 offspring on a mixed genetic background (designated B6;129).

Timed matings were performed by intercrossing *Lman1*^{+/−} mice. Embryos from each cross were harvested at 18.5 days postcoitus. A tail biopsy was obtained from each embryo for genotyping, and embryos were fixed in Z-Fix solution (Anatech LTD) for histology. All animals were housed according to the University of Michigan Unit of Laboratory Animal Medicine guidelines, and the University Committee on the Use and Care of Animals approved all studies.

Messenger RNA isolation and gene expression analysis

Total messenger RNA (mRNA) was isolated from tissues as previously described.[33] Reverse transcription and quantitative real-time PCR amplification were performed as previously described,[34] with primers listed in Table 1. Relative gene expression was calculated by using the $2^{-\Delta\Delta CT}$ method. β-actin and glyceraldehyde-3-phosphate dehydrogenase were used as internal controls. Two samples of each genotype were analyzed in triplicate for *Lman1* expression levels. The *Lman1* primers used for these assays were chosen based on the differences in the *Lman1*[cgt] and *Lman1*[gt1] alleles. The *Lman1*[cgt] allele has a gene trap in *Lman1* intron 1, whereas the *Lman1*[gt1] allele has a gene trap in intron 10. The 5′ end of the primer F6 matches exon 1 and the 3′ end matches exon 2, and thus it should only anneal to mRNA, correctly splicing these 2 exons (around the *Lman1*[cgt] gene trap). Similarly, the downstream F5-R5 primer pair anneals to any mRNA transcript in which splicing around the *Lman1*[gt1] gene trap occurs. Primer sequences for unfolded protein response genes were previously described and are listed in Table 1.[35]

Western blots

Western blot analysis of mouse tissues and plasma samples was performed as previously described.[5] Tissue lysate concentrations were determined by DC Protein Assay (Bio-Rad). Equal volumes of mouse plasma from individual animals were used for western blot analysis of plasma proteins. Antibodies used in the western blot experiments were: a mouse monoclonal antibody against murine glyceraldehyde-3-phosphate dehydrogenase
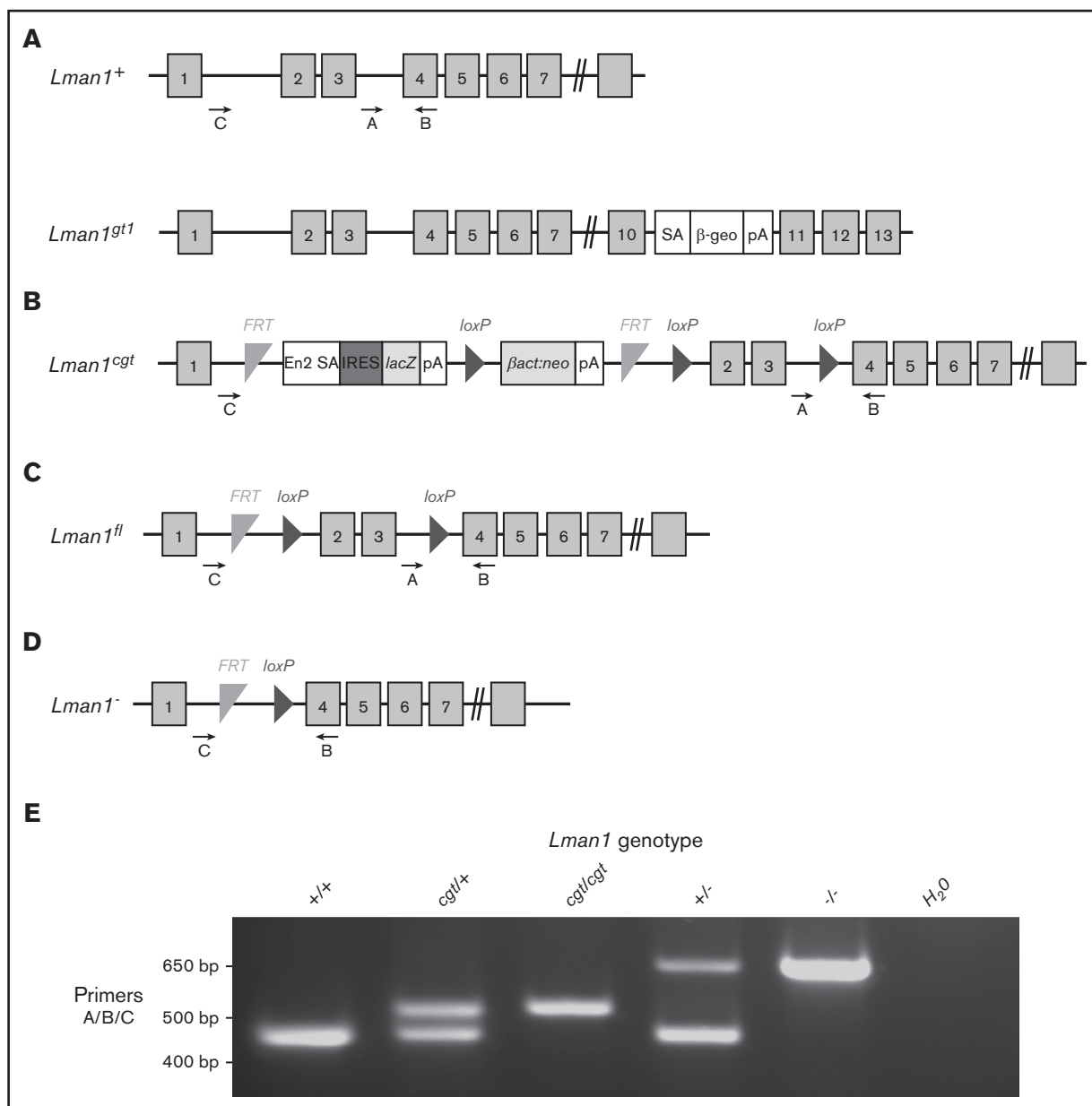
Figure 1. Schematic of *Lman1* mutant alleles. (A) *Lman1^gt1^* allele carries a gene trap insertion in intron 10.[28] (B) The *Lman1* conditional gene trap allele (*Lman1^cgt^*) contains a gene trap insertion in intron 1 flanked by 2 *FRT* sites. Mice carrying this allele were crossed to β-actin *FLP* transgenic mice.[5] Mice heterozygous for the resulting *Lman1* "floxed" allele (*Lman1^fl/+^*) (C) were crossed to *EIIA-Cre^+^* transgenic mice to excise exons 2 and 3, generating the *Lman1* null allele (*Lman1^−^*) (D). Gray blocks represent exons. A, B, and C represent genotyping primers. (E) A 3-primer PCR assay (primers A, B, and C) distinguishes the *Lman1^+^* (444 bp), *Lman1^cgt^* (508 bp), and *Lman1^−^* (635 bp) alleles. The *Lman1^fl^* allele (not shown in this image) also generates the same PCR product band as the *Lman1^cgt^* allele. βact:neo, human β-actin promoter-driven neomycin cassette; β-Geo, β-galactosidase-neo fusion; *cgt,* conditional gene trap; En2 SA, splice acceptor of mouse *En2* exon 2; *fl*, floxed; IRES, encephalomyocarditis virus (EMCV) internal ribosomal entry site; *lacZ, Escherichia coli* β-galactosidase gene; pA, poly-adenylation signal; SA, splice acceptor cassette.

(EMD Millipore), a mouse monoclonal antibody against murine RALA (Sigma-Aldrich), a chicken polyclonal antibody against murine A1AT (GenWay Biotech), a rabbit polyclonal antibody against human A1AT (Proteintech), and a rabbit polyclonal antibody against murine LMAN1 (Sigma-Aldrich). Horseradish peroxidase was detected by using an enhanced chemiluminescence kit (PerkinElmer). The fraction of A1AT retained in the ER (upper band:lower band in the same western blot lane)

in liver lysates was quantified by using an IRDye-conjugated secondary antibody (LI-COR Biosciences) and the Odyssey Infrared Imaging System, with analysis performed on the Odyssey CLx Image Studio program (LI-COR Biosciences). Densitometry quantification of the LMAN1 and A1AT western blots was performed with ImageJ software (https://imagej.nih.gov), with normalization to the respective control band in each lane.

Table 1. Primer sequences

Primer	5′ → 3′ Sequence
Genotyping primers	
Lman1 primer A	GGCTTTCTTGACACCTTCAATTTAA
Lman1 primer B	CCAAGTGAAGGGAAGACCATCAAGC
Lman1 primer C	GACCCCTAGTGACGGGTTCTTGTC
EIIA-Cre transgene Fwd	CCGCTGGAGATGACGTAGTT
EIIA-Cre transgene Rev	CGCATAACCAGTGAAACAGCATTGC
qRT-PCR primers	
Gapdh Fwd	TGTGTCCGTCGTGGATCTGA
Gapdh Rev	ACCACCTTCTTGATGTCATCATACTT
β-actin Fwd	CTAAGGCCAACCGTGAAAAG
β-actin Rev	GGGGTGTTGAAGGTCTCAAA
F5	ACGTGGTGAAGAGAGATATCGAC
R5	ACAAAGTGGATCGTGGATAGACA
F6	GCCCAGGCGGGGAATGCTATTCCAAG
R6	TCTCGAAGGCTGCTTTTGCTTTGGT
Aft6 Fwd	CTTCCTCCAGTTGCTCCATC
Aft6 Rev	CAACTCCTCAGGAACGTGCT
BiP Fwd	CATGGTTCTCACTAAAATGAAAGG
BiP Rev	GCTGGTACAGTAACAACTG
Chop Fwd	CTGCCTTTCACCTTGGAGAC
Chop Rev	CGTTTCCTGGGGATGAGATA
XBP total Fwd	AAGAACACGCTTGGGAATGG
XBP total Rev	ACTCCCCTTGGCCTCCAC
XBP spliced Fwd	GAGTCCGCAGCAGGTG
XBP spliced Rev	GTGTCAGAGTCCATGGGA

Tissue histology

Tissues for histologic examination were placed in Z-Fix solution (Anatech LTD) and prepared as previously described.[36,37] Histologic surveys (hematoxylin and eosin staining) were performed on adult $Lman1^{-/-}$ and $Lman1^{+/+}$ mouse tissues, as well as on embryos harvested from timed matings and newborn pups from $Lman1^{+/-}$ intercrosses, by a pathologist blinded to mouse genotype at the University of Michigan Pathology Cores for Animal Research, as previously described.[36,38] Images were taken by using an Olympus BX43 microscope and an Olympus DP72 camera. Kidney and lung images are magnified 40×, and heart and liver images are magnified 60×.

Measurement of FV and FVIII levels

Blood collection via inferior vena cava puncture and platelet-poor plasma isolation were performed as previously described.[5] Plasma FV and FVIII activity levels were determined in prothrombin time–based and partial thromboplastin time–based assays, respectively, as previously described.

Statistical analysis

A χ^2 test was used to evaluate statistical deviation from expected Mendelian ratios for the genotypes of offspring from the matings listed in Table 2 and for the genotype distributions listed in Table 3. Analysis of the FV and FVIII activity assays was performed by using the Student t test for comparison between 2 different genotypes and by one-way analysis of variance for comparisons of >2 groups. Statistical analysis of the ratios of post-ER A1AT:ER-retained A1AT for $Lman1$ mutant mice and wild-type control mice was performed by using the Student t test for comparison between different genotypes. $P < .05$ is considered statistically significant for these analyses; P values that are not statistically significant are abbreviated as "n.s." in the figures and legends.

Results

Reduced $Lman1$ expression results in dose-dependent decreases in FV and FVIII

$Lman1$ mRNA expression in the liver of $Lman1^{cgt/cgt}$ mice was reduced to ~4% to 6% of wild-type levels as measured by quantitative reverse transcription PCR (qRT-PCR) (Figure 2A-B), compared with <1% of wild type in liver mRNA from $Lman1^{gt1/gt1}$ mice. This low level of $Lman1$ mRNA expression likely results from a low level of alternative splicing around the $Lman1^{cgt}$ gene trap construct. Reduced levels of the expected truncated mRNA were detected in $Lman1^{gt1/gt1}$ mice when tested with the F6/R6 primer pair, consistent with nonsense-mediated decay of the $Lman1^{gt1}$ β-geo fusion mRNA compared with wild-type $Lman1$ mRNA.[39] Less than 1% of $Lman1$ mRNA expression distal to intron 10 was detected in the liver of $Lman1^{gt1/gt1}$ mice (primer pair F5/R5), consistent with a complete block of mRNA transcription distal to the gene trap insertion. An identical qRT-PCR study for $Lman1$ mRNA expression in kidney lysates of $Lman1^{cgt/cgt}$ mice was consistent with the liver expression levels, with reduction to ~6% to 8% of wild-type levels (Figure 2C-D). LMAN1 protein levels detected in liver lysates (Figure 3A) were consistent with the qRT-PCR results, with reduced levels in $Lman1^{cgt/cgt}$ (~15% of wild-type levels by densitometry of the western blot bands) and undetectable levels in $Lman1^{-/-}$ and $Lman1^{gt1/gt1}$ mice. Analysis of additional tissues from $Lman1^{cgt/cgt}$ mice exhibited consistently reduced LMAN1 relative to wild-type mice (Figure 3B).

To test the hypothesis that $Lman1$ expression levels correlate with secretion levels of LMAN1-dependent cargoes in a dose-dependent manner, we measured plasma activity levels of FV and FVIII, as well as relative levels of plasma and intracellular (hepatocyte) A1AT in mice homozygous for each of the $Lman1$ alleles. $Lman1^{-/-}$ and $Lman1^{gt1/gt1}$ mice on a C57BL/6J genetic

Table 2. Intercrosses of $Lman1$ mutant mice

Crosses	Strain	Genotype distribution at 3 wk, % (no. observed)		P, χ^2
		+/+ and +/−	−/−	
Expected %		75	25	
$Lman1^{gt1/+}$ x $Lman1^{gt1/+}$	C57BL/6J	83 (201)	17 (40)	<.003
$Lman1^{cgt/+}$ x $Lman1^{cgt/+}$	C57BL/6J	80 (107)	20 (27)	>.19
$Lman1^{+/-}$ x $Lman1^{+/-}$	C57BL/6J	83 (184)	17 (38)	<.007
Dead pups (<24 h)	C57BL/6J	50 (11)	50 (11)	<.007
$Lman1^{+/-}$ x $Lman1^{+/-}$	B6;129 mixed	76 (95)	24 (30)	>.79

The χ^2 test was based on an expected genotype ratio of 3:1, with $Lman1^{-/-}$ mice expected to represent 25% of the offspring from each mating, and all other genotypes cumulatively accounting for 75% of offspring.

blood advances

Table 3. Genotype distribution of pups from intercrosses of
***Lman1*$^{+/-}$ and *Mcfd2*$^{+/-}$ mice**

	Genotype		
	Lman1$^{-/-}$	*Lman1*$^{+/-}$ or *Lman1*$^{+/+}$	P, χ^2
Observed	48	217	<.01
Expected	66	199	
	Mcfd2$^{-/-}$	*Mcfd2*$^{+/-}$ or *Mcfd2*$^{+/+}$	
Observed	61	204	>.45
Expected	66	199	

Intercrosses between mice doubly heterozygous for *Lman1*$^-$ and *Mcfd2*$^-$ were performed to generate double-null *Lman1*$^{-/-}$ mice, *Mcfd2*$^{-/-}$ mice, and littermate controls; 265 mice of the 9 possible expected genotypes were generated (Table 3).

background or *Lman1*$^{-/-}$ mice on a mixed B6;129 genetic background (supplemental Figure 1) exhibited plasma FV and FVIII activity levels that are ~50% of wild-type levels, consistent with previous reports.[28] *Lman1*$^{-/-}$ mice (C57BL/6J) exhibit FV activity levels that are 48.7% ± 4.0% of wild-type levels ($P <$ .0001) but which are indistinguishable from the levels in *Lman1*$^{gt1/gt1}$ mice (54.4% ± 3.9%) (Figure 4A). FV activity levels of *Lman1*$^{+/-}$ mice are indistinguishable from wild-type mice, consistent with the autosomal recessive inheritance pattern of F5F8D. In contrast, the hypomorphic *Lman1*$^{cgt/cgt}$ mice exhibit intermediate levels of FV activity (67.1% ± 5.3%), significantly lower than those of wild-type mice ($P <$ .0004) but significantly higher than those of the complete null *Lman1*$^{-/-}$

mice ($P <$ .011). Data for FVIII activity levels in these different mouse genotypes were similar, as shown in Figure 4B. *Lman1*$^{-/-}$ mice (C57BL/6J) exhibit FVIII activity levels that are 49.2% ± 4.6% of wild-type levels ($P <$ .0001) but which are indistinguishable from the levels in *Lman1*$^{gt1/gt1}$ mice (49.5% ± 2.2%). FVIII activity levels of *Lman1*$^{+/-}$ mice are indistinguishable from those of wild-type mice. The hypomorphic *Lman1*^{cgt} mice exhibit intermediate levels of FVIII activity (62.8% ± 4.2%), significantly lower than those of wild-type mice ($P <$ .0001) but significantly higher than those of the complete null *Lman1*$^{-/-}$ mice ($P <$ .042). Heterozygous carriers of the *Lman1*^{cgt}, *Lman1*^{gt1}, or the *Lman1*$^-$ alleles exhibit FV and FVIII activity levels indistinguishable from those of control mice or from one another (supplemental Figure 2A-D), consistent with the autosomal recessive inheritance of F5F8D in humans, and with previously published reports in mice.[28]

A1AT accumulates in the ER of *Lman1*-deficient mice

It was previously shown that *Lman1*$^{gt1/gt1}$ liver extracts contain higher levels of intracellular A1AT, compared with wild-type control mice, despite their comparable steady-state plasma A1AT levels.[28] It was similarly shown, through endoglycosidase H digestion experiments, that the increased intracellular accumulation of A1AT in *Lman1*$^{gt/gt}$ mice is the result of ER retention of A1AT. Similar experiments were performed for the current study using liver extracts from wild-type, *Lman1*$^{cgt/cgt}$, *Lman1*$^{gt1/gt1}$, and *Lman1*$^{-/-}$ mice to determine if there is also a dose–response relationship between levels of *Lman1* expression and ER-to-Golgi transport of A1AT. As shown in Figure 5A, western blots

Figure 2. *Lman1* mRNA expression levels in *Lman1*$^{cgt/cgt}$ and *Lman1*$^{gt1/gt1}$ mice. (A-B) qRT-PCR of liver complementary DNA from *Lman1*$^{cgt/cgt}$ and *Lman1*$^{gt1/gt1}$ mice. (C-D) qRT-PCR of kidney complementary DNA from *Lman1*$^{cgt/cgt}$ mice. Three mice per genotype were used for qRT-PCR analysis. Horizontal bars represent means, and error bars represent standard error of the mean.
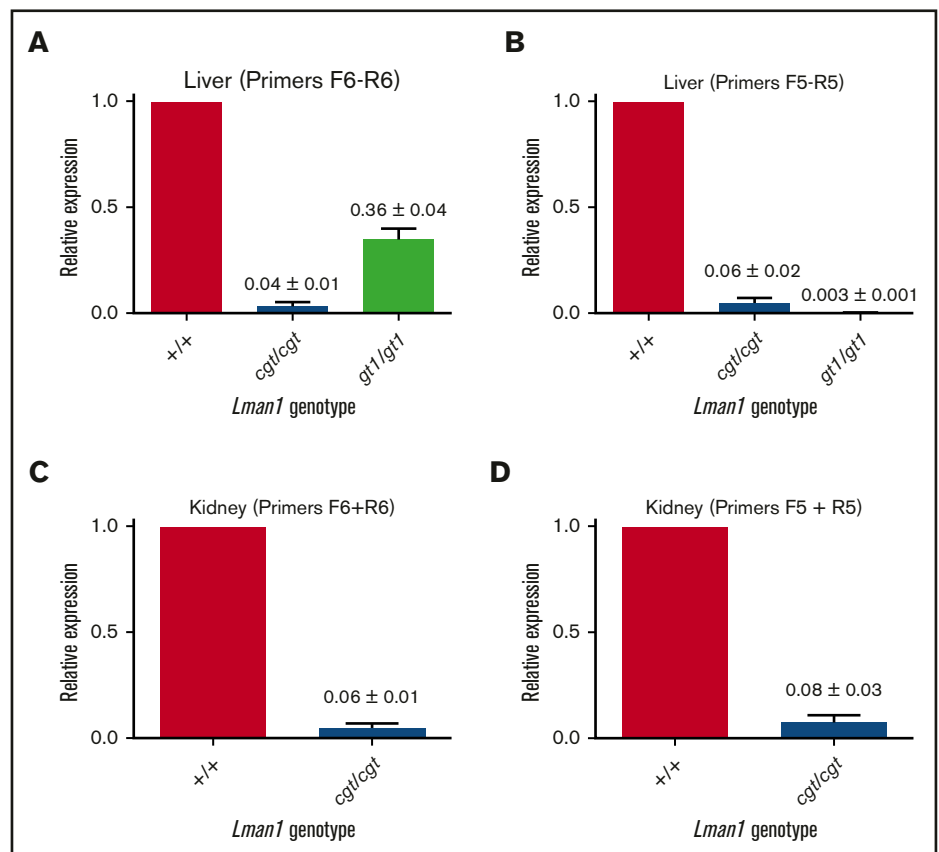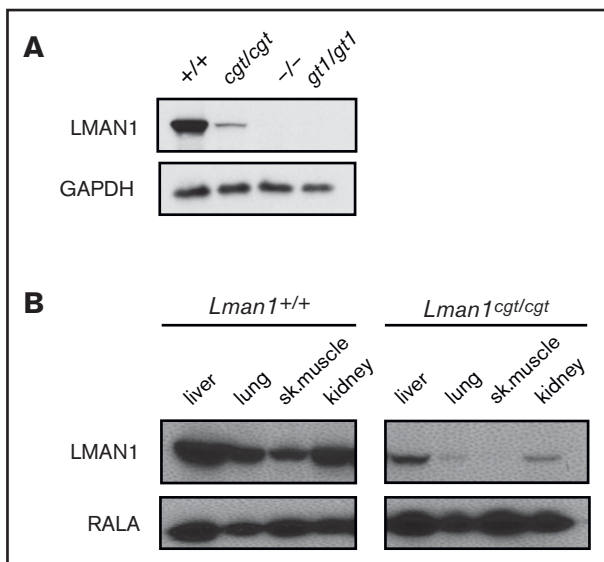
Figure 3. Western blot of LMAN1 expression in *Lman1* mutant mice. (A) Western blot of liver lysates from homozygote carriers of the *Lman1* mutant alleles: *Lman1*[cgt], *Lman1*^{−}, and *Lman1*[gt1]. (B) Western blot of multiple tissue lysates from wild-type and *Lman1*[cgt/cgt] mice. GAPDH, glyceraldehyde-3-phosphate dehydrogenase.

were performed to identify A1AT levels in 3 independent samples for each *Lman1* genotype. The A1AT antibody produces a doublet, with the top band corresponding to the A1AT that has been processed in the Golgi (the same size as the secreted plasma A1AT band); the lower band in the doublet corresponds to the ER-retained A1AT. This lower band was previously shown to be sensitive to endoglycosidase H digestion, consistent with retention in the ER.[28]

Consistent with the prior report for *Lman1*[gt1/gt1] mice, intracellular A1AT accumulation in hepatic lysates was observed in *Lman1*[cgt/cgt],

Lman1[gt1/gt1], and *Lman1*^{−/−} hepatocytes (Figure 5A). Compared with the high proportion of post-ER A1AT (upper band) in wild-type mice, LMAN1-deficient mouse hepatic lysates have lower levels of post-ER A1AT and higher levels of ER-retained A1AT (lower band). The upper and lower bands in each doublet were quantified, and the ratio of post-ER A1AT to ER-retained A1AT was calculated for each sample (Figure 5B). A ratio >1 indicates that the majority of the intracellular A1AT has reached the Golgi, whereas a ratio <1 indicates that the majority of the intracellular A1AT is retained in the ER. These ratios follow a similar dose–response relationship to the level of *Lman1* expression as observed for FV and FVIII plasma activity levels. The *Lman1*^{−/−} mice exhibit a statistically significantly lower ratio compared with wild-type mice (mean 0.50 ± 0.04 compared with 2.1 ± 0.2, respectively; $P < .0003$), and there was no difference between the *Lman1*^{−/−} and *Lman1*[gt1/gt1] mice. The hypomorphic *Lman1*[cgt/cgt] mice exhibit an intermediate ratio of post-ER A1AT:ER-retained A1AT, which is significantly lower than that in wild-type mice (0.73 ± 0.04 vs 2.1 ± 0.2; $P < .0007$) and significantly higher than that in *Lman1*^{−/−} null mice ($P < .02$); this finding, however, was not significantly different from that in *Lman1*[gt1/gt1] mice, consistent with an intermediate level of intracellular A1AT accumulation.

Although A1AT (and presumably other LMAN1 cargoes) accumulates in the ER in LMAN1-deficient mice, there is no difference in the expression level of multiple unfolded protein response genes in *Lman1*^{−/−} mice compared with wild-type control mice, consistent with a prior report (supplemental Figure 3).[28]

LMAN1 deficiency results in perinatal lethality with incomplete penetrance

Confirming our previous results,[28] intercrosses of *Lman1*[gt1/+] mice on a C57BL/6J genetic background resulted in reduced numbers of homozygous *Lman1*[gt1/gt1] mice at 3 weeks of age (17% observed vs 25% expected; $P < .003$) (Table 2). Similar incompletely penetrant lethality was observed for *Lman1*^{−/−} mice (from an
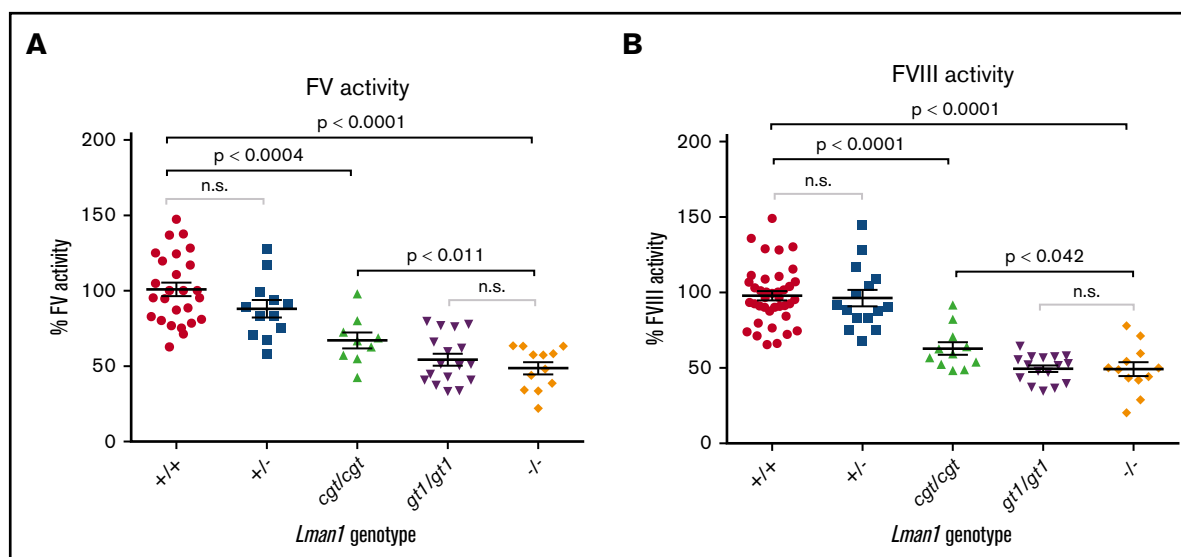
Figure 4. Plasma FV and FVIII activity levels for *Lman1* mutant mice (C57BL/6J background). (A) Plasma FV activity as percentage of wild-type. (B) Plasma FVIII activity as percentage of wild-type. Each symbol represents an individual animal. Horizontal lines indicate mean, and error bars indicate standard error of the mean for each genotype.
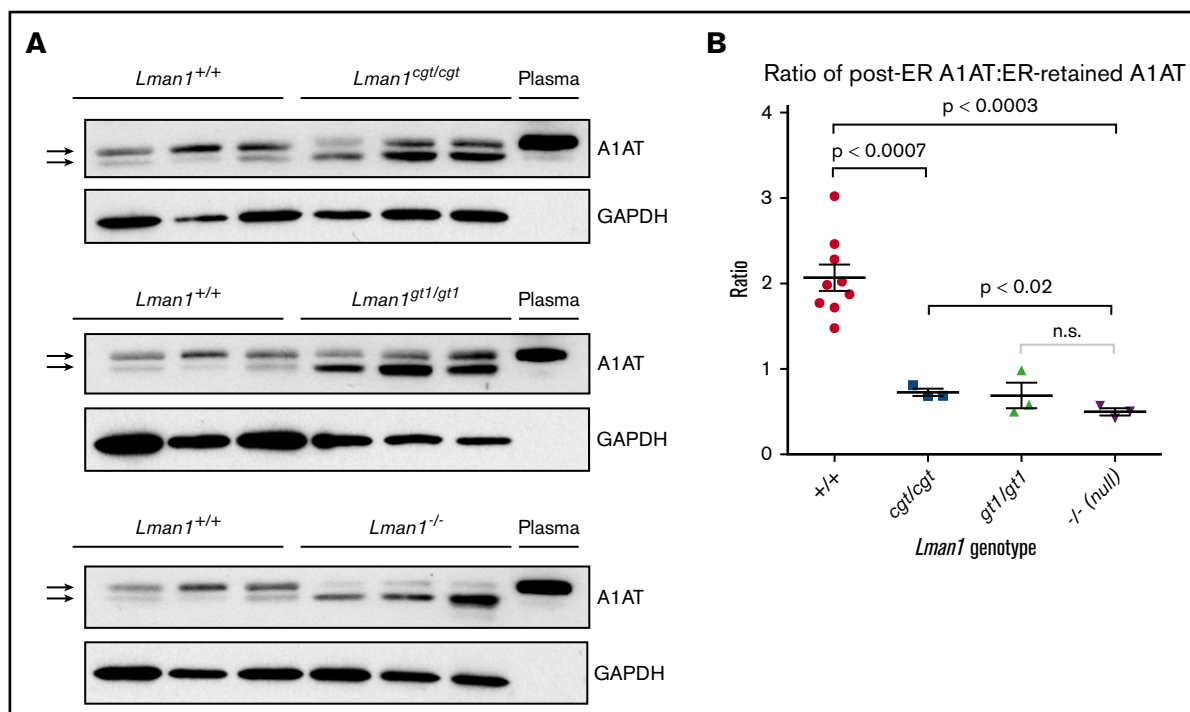
Figure 5. Western blot for A1AT in liver lysates. (A) Liver lysates prepared from $Lman1^{cgt/cgt}$, $Lman1^{gt1/gt1}$, $Lman1^{-/-}$, and $Lman1^{+/+}$ mice were analyzed by western blotting using an anti-A1AT antibody. The lower A1AT band corresponds to ER-retained A1AT (and was previously shown to be endoglycosidase H sensitive[28]). The upper A1AT band corresponds to post-ER A1AT and is comparable in molecular weight to secreted plasma A1AT. Each lane corresponds to an individual mouse. (B) The ratio of post-ER A1AT:ER-retained A1AT (upper band:lower band) in the hepatic lysates of each mouse as determined by densitometry; a ratio >1 indicates that the majority of the A1AT has been secreted beyond the ER, whereas a ratio <1 indicates that the majority of the A1AT is retained in the ER. Horizontal lines indicate the mean, and error bars indicate the standard error of the mean for each genotype.

$Lman1^{+/-}$ intercross) ($P < .007$). Genotyping of pups dying spontaneously on the first day of life revealed an excess of $Lman1^{-/-}$ pups (11 of 22; $P < .007$), consistent with perinatal lethality. No obvious histologic abnormalities were observed on necropsy of $Lman1^{-/-}$ pups and wild-type littermates euthanized at E18.5 to suggest a cause of death; histologic examination of adult $Lman1^{-/-}$ mice was also unremarkable (supplemental Figure 4). In contrast, the expected number of $Lman1^{cgt/cgt}$ mice at weaning was observed from an $Lman1^{cgt/+}$ intercross ($P > .19$). Similar to previously reported results for the $Lman1^{gt1}$ allele,[28] no perinatal lethality was observed for $Lman1^{-/-}$ pups on a mixed C57BL/6J-129S1/SvImJ genetic background ($P > .79$). Intercrosses between $Lman1^{+/-}/Mcfd2^{+/-}$ mice confirmed the partial perinatal lethality for the $Lman1^{-/-}$ but not the $Mcfd2^{-/-}$ genotype (Table 3).[32]

Discussion

We report the characterization of a series of gene-targeted $Lman1$ alleles directing gene expression levels ranging from 0% to 7% of wild type, as confirmed by qRT-PCR and western blot expression studies in multiple tissues. The observation of similar plasma FV and FVIII levels in $Lman1^{gt1/gt1}$ and $Lman1^{-/-}$ mice excludes trace residual LMAN1 expression from the $Lman1^{gt1}$ allele as the explanation for more modest reductions in FV and FVIII in LMAN1-deficient mice compared with humans.[28] These findings also suggest that, at least in mice, an LMAN1-independent mechanism for FV and FVIII secretion may account for the residual ~50% levels in LMAN1 null animals. This alternative

mechanism could be mediated by another cargo receptor, potentially a paralog of LMAN1 (eg, ERGL). Such an alternative cargo receptor could be expressed constitutively, or only induced in the absence of LMAN1. The confirmation of the previously reported perinatal, strain-specific lethality[28] with an independent $Lman1^-$ allele also excludes a passenger gene effect[40] not due to LMAN1 deficiency as the cause of lethality in $Lman1^{gt1/gt1}$ mice. In contrast, mice homozygous for the hypomorphic $Lman1^{cgt}$ allele are not significantly reduced in number. Because fetal loss would not be expected to result from moderate FV and FVIII deficiency, these data suggest the existence of another, as yet unknown, critical LMAN1-dependent cargo(s). The lack of evidence for perinatal loss in human F5F8D patients despite much greater reductions in FV and FVIII,[16] together with normal survival of $Lman1^{-/-}$ mice on a mixed genetic background, are consistent with enhanced susceptibility of inbred mice to reduced ER exit of a key LMAN1 cargo. However, differences in the repertoire of LMAN1 cargoes between mouse and human cannot be excluded.

We report a dose–response relationship between the levels of LMAN1 expression and the steady-state plasma levels of FV and FVIII. These results are surprising given the apparent enrichment for null mutations among $LMAN1$ alleles identified in F5F8D patients,[41] which suggested that even low levels of residual LMAN1 function are sufficient to support normal FV and FVIII secretion. Taken together, these observations raise the possibility that human subjects with hypomorphic $LMAN1$ mutations and residual LMAN1 activity might present with more modest reductions in FV and FVIII,

potentially resulting in only mild bleeding. Such mild disease could potentially have eluded clinical detection or a specific genetic diagnosis to date. Our results thus suggest considering genetic testing in patients with more modestly reduced FV and FVIII levels than those typically associated with F5F8D. These findings also suggest that therapeutic targeting of LMAN1 to reduce FV and FVIII levels as an anticoagulant strategy may only require partial inhibition of LMAN1 function.

Authorship

Contribution: L.A.E., R.N.K., and D.G. designed the research; L.A.E. and R.N.K. performed the experiments; L.A.E., R.N.K., B.Z., and D.G. analyzed the data; L.A.E., R.N.K, and D.G. wrote the manuscript; and all authors reviewed and commented on the manuscript.

Conflict-of-interest disclosure: The authors declare no competing financial interests.

ORCID profiles: L.A.E., 0000-0002-7373-2056; R.N.K., 0000-0003-2539-5953; D.G., 0000-0002-6436-8942.

Correspondence: David Ginsburg, Life Sciences Institute, University of Michigan, 210 Washtenaw Ave, Ann Arbor, MI 48109; e-mail: ginsburg@umich.edu.

References

1. Khoriaty R, Vasievich MP, Ginsburg D. The COPII pathway and hematologic disease. *Blood*. 2012;120(1):31-38.

2. Camire RM, Pollak ES, Kaushansky K, Tracy PB. Secretable human platelet-derived factor V originates from the plasma pool. *Blood*. 1998;92(9):3035-3041.

3. Gould WR, Simioni P, Silveira JR, Tormene D, Kalafatis M, Tracy PB. Megakaryocytes endocytose and subsequently modify human factor V in vivo to form the entire pool of a unique platelet-derived cofactor. *J Thromb Haemost*. 2005;3(3):450-456.

4. Sun H, Yang TL, Yang A, Wang X, Ginsburg D. The murine platelet and plasma factor V pools are biosynthetically distinct and sufficient for minimal hemostasis. *Blood*. 2003;102(8):2856-2861.

5. Everett LA, Cleuren AC, Khoriaty RN, Ginsburg D. Murine coagulation factor VIII is synthesized in endothelial cells. *Blood*. 2014;123(24):3697-3705.

6. Fahs SA, Hille MT, Shi Q, Weiler H, Montgomery RR. A conditional knockout mouse model reveals endothelial cells as the principal and possibly exclusive source of plasma factor VIII. *Blood*. 2014;123(24):3706-3713.

7. Nichols WC, Seligsohn U, Zivelin A, et al. Mutations in the ER-Golgi intermediate compartment protein ERGIC-53 cause combined deficiency of coagulation factors V and VIII. *Cell*. 1998;93(1):61-70.

8. Zhang B, Cunningham MA, Nichols WC, et al. Bleeding due to disruption of a cargo-specific ER-to-Golgi transport complex. *Nat Genet*. 2003;34(2):220-225.

9. Hauri H, Appenzeller C, Kuhn F, Nufer O. Lectins and traffic in the secretory pathway. *FEBS Lett*. 2000;476(1-2):32-37.

10. Fiedler K, Simons K. A putative novel class of animal lectins in the secretory pathway homologous to leguminous lectins. *Cell*. 1994;77(5):625-626.

11. Itin C, Roche AC, Monsigny M, Hauri HP. ERGIC-53 is a functional mannose-selective and calcium-dependent human homologue of leguminous lectins. *Mol Biol Cell*. 1996;7(3):483-493.

12. Zheng C, Page RC, Das V, et al. Structural characterization of carbohydrate binding by LMAN1 protein provides new insight into the endoplasmic reticulum export of factors V (FV) and VIII (FVIII). *J Biol Chem*. 2013;288(28):20499-20509.

13. Zheng C, Liu HH, Yuan S, Zhou J, Zhang B. Molecular basis of LMAN1 in coordinating LMAN1-MCFD2 cargo receptor formation and ER-to-Golgi transport of FV/FVIII. *Blood*. 2010;116(25):5698-5706.

14. Lee MC, Miller EA, Goldberg J, Orci L, Schekman R. Bi-directional protein transport between the ER and Golgi. *Annu Rev Cell Dev Biol*. 2004;20(1):87-123.

15. Miller EA, Beilharz TH, Malkus PN, et al. Multiple cargo binding sites on the COPII subunit Sec24p ensure capture of diverse membrane proteins into transport vesicles. *Cell*. 2003;114(4):497-509.

16. Zhang B, Spreafico M, Zheng C, et al. Genotype-phenotype correlation in combined deficiency of factor V and factor VIII. *Blood*. 2008;111(12):5592-5600.

17. Zhang B, McGee B, Yamaoka JS, et al. Combined deficiency of factor V and factor VIII is due to mutations in either LMAN1 or MCFD2. *Blood*. 2006;107(5):1903-1907.

18. Zheng C, Zhang B. Combined deficiency of coagulation factors V and VIII: an update. *Semin Thromb Hemost*. 2013;39(6):613-620.

19. Nufer O, Kappeler F, Guldbrandsen S, Hauri HP. ER export of ERGIC-53 is controlled by cooperation of targeting determinants in all three of its domains. *J Cell Sci*. 2003;116(Pt 21):4429-4440.

20. Yamada T, Fujimori Y, Suzuki A, et al. A novel missense mutation causing abnormal LMAN1 in a Japanese patient with combined deficiency of factor V and factor VIII. *Am J Hematol*. 2009;84(11):738-742.

21. Seligsohn U, Zivelin A, Salomon O. Inherited deficiencies of coagulation factors II, V, VII, X, XI, and XIII and combined deficiencies of factors V and VIII and of the vitamin K-dependent factors. *Williams Hematology*. 8th ed.. New York, NY: The McGraw-Hill Companies; 2010.

22. Nyfeler B, Reiterer V, Wendeler MW, et al. Identification of ERGIC-53 as an intracellular transport receptor of alpha1-antitrypsin. *J Cell Biol*. 2008; 180(4):705-712.

23. Vollenweider F, Kappeler F, Itin C, Hauri HP. Mistargeting of the lectin ERGIC-53 to the endoplasmic reticulum of HeLa cells impairs the secretion of a lysosomal enzyme. *J Cell Biol*. 1998;142(2):377-389.

24. Appenzeller C, Andersson H, Kappeler F, Hauri HP. The lectin ERGIC-53 is a cargo transport receptor for glycoproteins. *Nat Cell Biol*. 1999;1(6): 330-334.

25. Chen Y, Hojo S, Matsumoto N, Yamamoto K. Regulation of Mac-2BP secretion is mediated by its N-glycan binding to ERGIC-53. *Glycobiology*. 2013; 23(7):904-916.

26. Duellman T, Burnett J, Shin A, Yang J. LMAN1 (ERGIC-53) is a potential carrier protein for matrix metalloproteinase-9 glycoprotein secretion. *Biochem Biophys Res Commun*. 2015;464(3):685-691.

27. Fu YL, Zhang B, Mu TW. LMAN1 (ERGIC-53) promotes trafficking of neuroreceptors. *Biochem Biophys Res Commun*. 2019;511(2):356-362.

28. Zhang B, Zheng C, Zhu M, et al. Mice deficient in LMAN1 exhibit FV and FVIII deficiencies and liver accumulation of α1-antitrypsin. *Blood*. 2011;118(12): 3384-3391.

29. Klaus JP, Eisenhauer P, Russo J, et al. The intracellular cargo receptor ERGIC-53 is required for the production of infectious arenavirus, coronavirus, and filovirus particles. *Cell Host Microbe*. 2013;14(5):522-534.

30. Hao H, Gregorski J, Qian H, et al. In vivo function of the ER-Golgi transport protein LMAN1 in photoreceptor homeostasis. *Adv Exp Med Biol*. 2014;801: 395-399.

31. Roeckel N, Woerner SM, Kloor M, et al. High frequency of LMAN1 abnormalities in colorectal tumors with microsatellite instability. *Cancer Res*. 2009; 69(1):292-299.

32. Zhu M, Zheng C, Wei W, Everett L, Ginsburg D, Zhang B. Analysis of MCFD2- and LMAN1-deficient mice demonstrates distinct functions in vivo. *Blood Adv*. 2018;2(9):1014-1021.

33. Adams EJ, Chen XW, O'Shea KS, Ginsburg D. Mammalian COPII coat component SEC24C is required for embryonic development in mice. *J Biol Chem*. 2014;289(30):20858-20870.

34. Khoriaty R, Vasievich MP, Jones M, et al. Absence of a red blood cell phenotype in mice with hematopoietic deficiency of SEC23. *Mol Cell Biol*. 2014; 34(19):3721-3734.

35. Han J, Kaufman RJ. Measurement of the unfolded protein response to investigate its role in adipogenesis and obesity. *Methods Enzymol*. 2014;538: 135-150.

36. Khoriaty R, Everett L, Chase J, et al. Pancreatic SEC23B deficiency is sufficient to explain the perinatal lethality of germline SEC23B deficiency in mice. *Sci Rep*. 2016;6(1):27802.

37. Khoriaty R, Hesketh GG, Bernard A, et al. Functions of the COPII gene paralogs SEC23A and SEC23B are interchangeable in vivo. *Proc Natl Acad Sci U S A*. 2018;115(33):E7748-E7757.

38. Khoriaty R, Vogel N, Hoenerhoff MJ, et al. SEC23B is required for pancreatic acinar cell function in adult mice. *Mol Biol Cell*. 2017;28(15):2146-2154.

39. Hentze MW, Kulozik AE. A perfect message: RNA surveillance and nonsense-mediated decay. *Cell*. 1999;96(3):307-310.

40. Westrick RJ, Mohlke KL, Korepta LM, et al. Spontaneous Irs1 passenger mutation linked to a gene-targeted SerpinB2 allele. *Proc Natl Acad Sci U S A*. 2010;107(39):16904-16909.

41. Zhang B. Recent developments in the understanding of the combined deficiency of FV and FVIII. *Br J Haematol*. 2009;145(1):15-23.